



Multi-objective Optimization of HMGF Process Parameters for Manufacturing AA6063 Stepped Tubes using FEM-RSM

M. Rajae^a, S. J. Hosseinipour^{*b}, H. Jamshidi Aval^b

^a Department of Mechanics, Faculty of Neyshabour, Khorasan Razavi Branch, Technical and Vocational University, Neyshabour, Iran

^b Research Center for Advanced Processes of Materials Forming, Babol Noshirvani University of Technology, Babol, Iran

PAPER INFO

Paper history:

Received 11 December 2020

Received in revised form 16 March 2021

Accepted 26 March 2021

Keywords:

AA6063 Alloy Tube

Hot Metal Gas Forming

Response Surface Methodology

Finite Elements Analysis

Optimization

ABSTRACT

In this paper, the loading path was optimized in hot metal gas forming (HMGF) process for making AA6063 cylindrical stepped tubes. For this purpose, the response surface method (RSM) and finite element method (FEM) were applied using Design-Expert and ABAQUS softwares, respectively. The parameters of internal pressure, pressure rate, axial feeding, and punch speed were examined based on the central-composite design in the three levels. The maximum die filling and the minimum tube thinning percentages were selected as the objective functions. The analysis of variance showed that the axial feeding, internal pressure, and their interaction were the most significant parameter in the die filling and tube thinning. The optimum loading path at the temperature of 550 °C was obtained at pressure of about 7 bars, pressure rate of 0.01 bar/s, axial feeding of 7 mm from each side and punch speed of 0.02 mm/s. Experimental tests were performed for the specified process parameters. The numerical results were validated by experimental testing.

doi: 10.5829/ije.2021.34.05b.25

1. INTRODUCTION

Although the deformation of high-strength and lightweight alloys are difficult, their applications are widely expanded in various industries, including the aerospace and automotive industries [1-5]. Hot metal gas forming (HMGF) is a high temperature forming processes, which serves for forming metal sheets and tubes using gas with low pressure. This technique is used for the deformation of alloys that have limited formability at ambient temperature [6, 7]. Paul et al. [8] developed a one-step HMGF process to produce an exhaust component made of titanium grade 2. Mosel et al. [9] described a process chain for the HMGF process to produce exhaust components made of ferritic stainless steel 1.4509. Talebi-Anaraki et al. [10] used a flame heating technique for forming aluminum alloy tubes by HMGF process. Rajae et al. [11] showed that the effect of HMGF parameters on the deformation behavior is complicated, and it is necessary to obtain their optimal

range. Response surface methodology (RSM) is one of the modeling methods, which uses mathematical and statistical techniques, leading to the reduction of costly experimental tests and the prediction of the optimized trend of the process. Many research works were carried out using this method to optimize parameters in various processes [12, 13]. Here are a few of them on the subject of forming metal tubes. Alaswad et al. [14] investigated the effect of geometric parameters on tube thickness and protrusion height in the hydroforming process of a T-shaped two-layer tube. The finite element model and RSM were used in this research. Chebbah et al. [15] optimized the loading path in the tube hydroforming process using a reverse finite element simulation method and RSM based on scattering approximation. The optimization purpose was to minimize the probability of some defects like necking and wrinkling. To search the global optimum of the objective function, they used the sequential quadratic programming (SQP) algorithm. Kadhodayan et al. [16] determined the mathematical

*Corresponding Author Institutional Email: j.hosseini@nit.ac.ir (S. J. Hosseinipour)

model between force variables and ductility using statistical analysis and the simulation of the tube hydroforming process. They acquired optimal loading curves for the production of T-shaped parts by applying the mathematical models initiated from an evolution algorithm. Safari et al. [17] maximized the convolution height and thickness of bellows congress parts by applying the mathematical models initiated from RSM. They reported that an increase in the convolution height and decrease in the thickness of the top point of bellows congress will occur by increasing the internal pressure and die stroke. Ahmadi Brooghani et al. [18] used a statistical manner established upon finite element simulation to find the optimal loading path. The exact finite element model of the forming process was prepared, and the created model verified in comparison with the experimental specimen. Huang et al. [19] optimized the loading path in the hydroforming of a T-shaped tube based on the response surface and non-probabilistic methods. The purpose of this research was to achieve the maximum protrusion and minimum thinning ratio with optimization of pressure path. Ge et al. [20] recommended a multi-objective optimization method for determining the parameters related to the hydroforming process of the tube using a differential evolution algorithm. They used several finite element simulations to set up a least-squares support vector machine-based on response surface model.

Studies show that little research carried out to find the optimal loading path of the HMGF process, and also most of the research was done on the tubes with specific geometrical properties. In this paper, optimization was performed using RSM and FEM to obtain the highest die filling and lowest tube thinning percentages for fabricating AA6063 cylindrical stepped tubes by the HMGF process.

2. MATERIALS AND METHODS

2. 1. Process Description and Simulation

AA6063 tube with a diameter of 25 mm and a thickness of 1.3 mm was employed. Figure 1 shows the die geometry, which the die diameter was 32 mm, and the length of the deformation zone was 60 mm. The axial feeding was carried out from the both sides of the die by two step-motors, and an air compressor was used to applying internal pressure. Uniform heating was created by applying resistance heaters inside the die and tube.

As shown in Figure 2, a one-fourth model was considered to simulate the process with ABAQUS finite element software. The tube was modeled deformable by C3D8R element with a mesh size of $1 \times 1 \times 0.43 \text{ mm}^3$, and the die was modeled as discrete rigid by R3D4 element. A distributed load was used to apply the effect of gas pressure, and the process was considered as an isotherm

process. A friction coefficient of 0.5 was used for contact surfaces [21, 22]. More details about the experiments and simulations are found in literature [10].

2. 2. Response Surface Methodology (RSM)

RSM was used to optimize the process parameters. The level of variables was specified, and then a matrix of the experiments was obtained based on the standard models. Afterward, the quadratic regression model and the mutual effect of the parameters were estimated using the analysis of variance (ANOVA). Finally, the optimal model was identified.

The process parameters, including internal pressure, pressure rate, axial feeding, and punch speed, were selected as independent variables. The forming temperature was constant at $550 \text{ }^\circ\text{C}$ during the process. The first objective function was the highest die filling percentage, which was defined as follows:

$$\text{Obj}_{\text{filling}} (\%) = \frac{V_s}{V_d} \times 100 \quad (1)$$

where V_d and V_s denoted the volume of the die and the specimen, respectively. The second objective function was the lowest tube thinning percentage, which was defined as follows:

$$\text{Obj}_{\text{thinning}} (\%) = \frac{t_0 - t_{\text{min}}}{t_0} \times 100 \quad (2)$$

where t_0 and t_{min} were the initial and minimum thickness of the tube, respectively.

Design-Expert software was used for the test design. Table 1 presents the independent variables, which

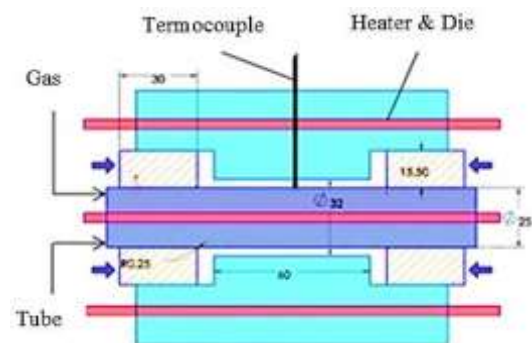


Figure 1. The die geometry, heaters, and tube (dimension in mm)

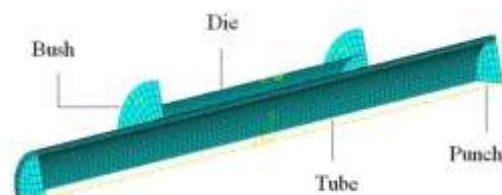


Figure 2. Finite element simulation model

evaluated at three levels based on the central composite design (CCD), and the matrix related to the test design is presented in Table 2.

3. RESULTS AND DISCUSSION

3.1. Statistical analysis Twenty five tests were obtained considering four continuous variables,

TABLE 1. The studied variables and their levels

Forming Parameters	Symbol	-1	0	1
Pressure (bar)	P	5	7	9
Pressure Rate (bar/s)	\dot{P}	0.01	0.03	0.05
Axial feed (mm)	X	0	3.5	7
Punch speed (mm/s)	V	0.01	0.03	0.05

TABLE 2. The design matrix of experiments

No.	P (bar)	\dot{P} (bar/s)	X (mm)	V (mm/s)	Filling (%)	Thinning (%)	Condition
1	5	0.01	0	0.01	-	-	Not filled
2	9	0.01	0	0.01	27.4	10.8	Ruptured
3	5	0.05	0	0.01	-	-	Not filled
4	9	0.05	0	0.01	11.58	4.97	Ruptured
5	5	0.01	7	0.01	82.72	8.98	Accepted
6	9	0.01	7	0.01	84.39	9.12	Accepted
7	5	0.05	7	0.01	89.22	14.62	Accepted
8	9	0.05	7	0.01	18.74	2.39	Ruptured
9	5	0.01	0	0.05	-	-	Not filled
10	9	0.01	0	0.05	27.77	11.2	Ruptured
11	5	0.05	0	0.05	-	-	Not filled
12	9	0.05	0	0.05	9.42	3.67	Ruptured
13	5	0.01	7	0.05	42.41	-0.02	Wrinkled
14	9	0.01	7	0.05	68.95	7.16	Wrinkled
15	5	0.05	7	0.05	72.67	4.3	Accepted
16	9	0.05	7	0.05	71.23	6.38	Ruptured
17	5	0.03	3.5	0.03	32.98	4.32	Accepted
18	9	0.03	3.5	0.03	79.28	8.46	Accepted
19	7	0.01	3.5	0.03	73.58	14.21	Accepted
20	7	0.05	3.5	0.03	69.27	12.26	Accepted
21	7	0.03	0	0.03	15.81	7.82	Accepted
22	7	0.03	7	0.03	81.98	6.44	Accepted
23	7	0.03	3.5	0.01	82.84	14.57	Accepted
24	7	0.03	3.5	0.05	73.04	13.04	Accepted
25	7	0.03	3.5	0.03	71.32	10.6	Accepted

including pressure, pressure rate, axial feed on each side, and punch speed, where the results are reported in Table 2. The diagrams related to the main effect of the four variables mentioned above on the die filling percentage and the thinning percentage can be observed in Figure 3. For the die filling percentage, the effect of the axial feed on each side was positive, meaning that by increasing this variable, the filling percentage is increased. The material flow to the die is facilitated by increasing the axial feed, causing the filling percentage to be increased. When the punch speed and pressure rate increased, the material flow does not have sufficient time to enter the die; therefore, the filling percentage is reduced. Increasing the pressure up to 7 bars leads to the enhancement of the die filling. However, increasing the pressure more than 7 bars leads to the collision of the tube with the die wall, and as a result of the generated friction, the filling percentage will decrease. About the effects of the pressure and axial feed on the thinning percentage, it can be seen that the effects of these two parameters on the thinning percentage are similar, meaning that the thinning percentage will increase first, and then, it will decrease by increasing these two parameters. Increasing

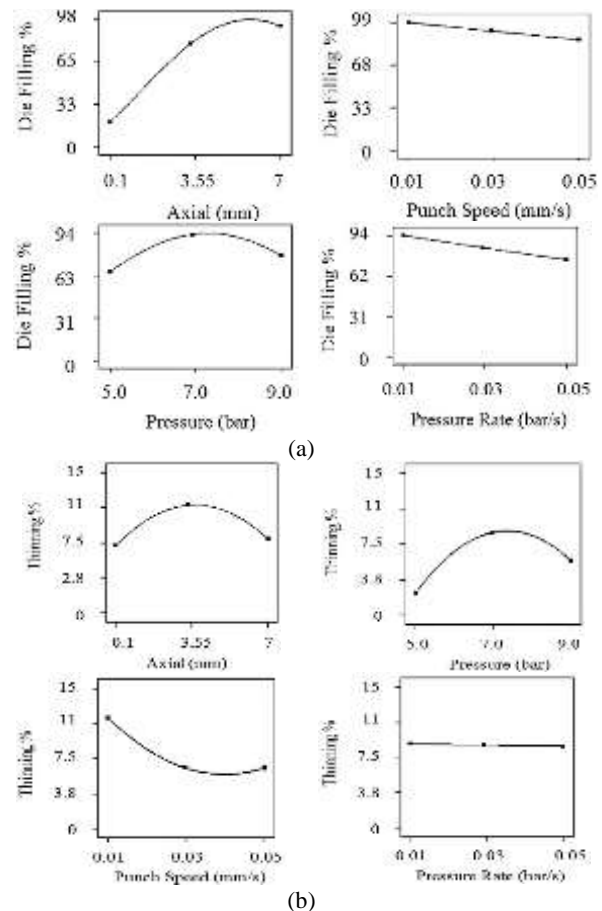


Figure 3. The effect of HMGF parameters on; a) die filling percent, and b) thinning percent

the pressure leads to the deformation of the tube inside the die cavity. Therefore, the thinning percentage of the die in the die cavity area will increase. However, due to the collision of the tube to the die surface, with a further increase in the pressure, the material flow becomes more difficult, and the thinning percentage will be reduced. Due to the formation of wrinkles in the tube, the excessive increase in the axial feed prevents the material to flow easily during the forming process, and the thinning percentage decrease. As can be seen, while the impact of the pressure applying speed on the thinning percentage is insignificant, the thinning percentage decreased by increasing the punch speed due to the generation of non-uniform flows inside the tube.

The results of the statistical investigation on the filling percentage based on different models are presented in Table 3. P-value is used to make sure of the accuracy of the model. The smaller the P-value (the significance value), the better the result fitting of the proposed model. Models and parameters that have P values less than 0.05 can statistically predict the data with errors of less than 5%. Due to the P-value, the quadratic equation was chosen as the most convenient model for the data fitting. Also, some of the statistical data related to the mentioned model, such as the coefficient of determination and the standard deviation, are briefly shown. If two parameters have equal significance value, the parameter that has a higher F-value (the test statistic) is more important. In Table 4, the results of the statistical investigation on the thinning percentage based on different models are presented. Here, the quadratic equation was also chosen as the most convenient model for the data fitting due to the P-value.

After choosing the quadratic equation as the proper model for the die filling, the ANOVA variance analysis was carried out, where the results are shown in Table 5.

TABLE 3. Statistical data of filling percentage based on different models

Source	SS	DF	MS	F value	P value	
Mean vs Total	1297.08	1	1297.08			
Linear vs Mean	142.41	4	35.6	8.33	0.0002	
2FI vs Linear	30.47	6	5.08	1.26	0.3204	
Quadratic vs 2FI	66.32	4	16.58	24.57	< 0.0001	Suggested
Cubic vs Quadratic	9.22	8	1.15	8.92	0.0046	Aliased
Residual	0.9	7	0.13			
Total	1546.4	30	51.55			

TABLE 4. Statistical data of thinning percentage based on different models

Source	SS	DF	MS	F value	p value	
Mean vs Total	1755.49	1	1755.49			
Linear vs Mean	105.66	4	2.64E+1	1.28	0.3046	
2FI vs Linear	184.2	6	3.07E+1	1.76	0.1622	
Quadratic vs 2FI	279.39	4	69.85	19.92	< 0.0001	Suggested
Cubic vs Quadratic	4.4E+1	8	5.53E+0	4.61	0.0294	Aliased
Residual	8.4E+0	7	1.20E+0			
Total	2377.3	30	79.24			

It can be observed that the two linear effects of pressure (P), and axial feeding (X) as well as their quadratic effects, and the two mutual effects of PX and P² are meaningful to the die filling. According to the ANOVA results, the parameters of axial feeding (X) and the mutual effect of PX have the most significant impact on the die filling. The obtained results indicated that the fitted quadratic model corresponds to the experimental data with a reliability coefficient of more than 93% (R²>93). After statistical analysis of the simulated data, the mathematical model (Eq. 3) presented using the four parameters, including pressure, pressure rate, axial feed on each side, and punch speed, to predict the value of the filling percentage.

$$\begin{aligned}
 (\% \text{ Die Filling})^{0.5} = & -17.69 + 5.40 P + 73.52 \dot{P} \\
 & + 3.05 X - 103.28 V - 17.33 P\dot{P} - 0.15 PX + 10.10 \\
 & PV + 975.91 \dot{P}V - 0.31 P^2 - 0.17 X^2
 \end{aligned} \tag{3}$$

Also, after selecting the quadratic model as the proper model for the thinning percentage, the ANOVA variance analysis was carried out, where the results are given in Table 6. It is seen that the three linear effects of pressure (P), axial feeding (X), and punch speed (V) as well as their quadratic effects, and the three mutual effects of P², PX, and PV are meaningful to the tube thinning. According to the ANOVA results, the parameters of pressure (P) and the mutual effect of PX have the most significant impact on the tube thinning. Moreover, after the statistical analysis of the simulated data, the following mathematical model is presented to predict the thinning percentage.

$$\begin{aligned}
 \% \text{ Thinning} = & -59.48 + 18.80 P + 250.91 \dot{P} + 4.74617 \\
 & X - 634.55 V - 48.25 P\dot{P} - 0.29 PX + 31.88 PV + 14.35 \\
 & \dot{P}X - 14.78 XV - 1.17 P^2 - 0.33 X^2 + 6814.91 V^2
 \end{aligned} \tag{4}$$

TABLE 5. The ANOVA results for the die filling percentage

	SS	DF	MS	F Value	P Value
Model	238.86	10	23.89	43.37	< 0.0001
P	9.79	1	9.79	17.78	0.0005
\dot{p}	2.48	1	2.48	4.50	0.0474
X	130.07	1	130.07	236.17	< 0.0001
V	0.076	1	0.076	0.14	0.7140
$P\dot{P}$	7.69	1	7.69	13.97	0.0014
PX	17.54	1	17.54	31.85	< 0.0001
PV	2.61	1	2.61	4.75	0.0421
$\dot{P}V$	2.44	1	2.44	4.43	0.0489
P^2	5.14	1	5.14	9.33	0.0065
X^2	14.18	1	14.18	25.75	< 0.0001
Residual	10.46	19	0.55		
Lack of Fit	10.46	14	0.75		
Pure Error	0.000	5	0.000		
Cor Total	249.32	29			

R² =95.8 %
R²(adj) = 93.59 %

Confirmation charts were utilized to determine the suitability of the filling percentage and thinning percentage regression models. Figure 4 shows the images of the actual values and the predicted values for each response. The straight line with a 45-degree angle represents the model, and the square dots represent the results obtained from the tests. The closer the dots to the line, the higher the accuracy of the model. This diagram confirms that the selected model describes the experimental values relatively well because the dots are around a line with a constant slope.

TABLE 6. The ANOVA results for the tube thinning percentage

	SS	DF	MS	F Value	P Value
Model	561.52	12	46.79	13.19	< 0.0001
P	52.93	1	52.93	14.92	0.0013
\dot{p}	9.29	1	9.29	2.62	0.1241
X	21.71	1	21.71	6.12	0.0242
V	21.73	1	21.73	6.12	0.0242
$P\dot{P}$	59.60	1	59.60	16.80	0.0007
PX	65.71	1	65.71	18.52	0.0005

PV	26.02	1	26.02	7.33	0.0149
$\dot{P}V$	15.68	1	15.68	4.42	0.0508
XV	16.64	1	16.64	4.69	0.0449
P^2	62.42	1	62.42	17.59	0.0006
X^2	44.39	1	44.39	12.51	0.0025
V^2	21.09	1	21.09	5.94	0.0260
Residual	60.33	17	3.55		
Lack of Fit	60.33	12	5.03		
Pure Error	0.000	5	0.000		
Cor Total	621.84	29			

R² =90.94 %
R²(adj)= 86.47 %

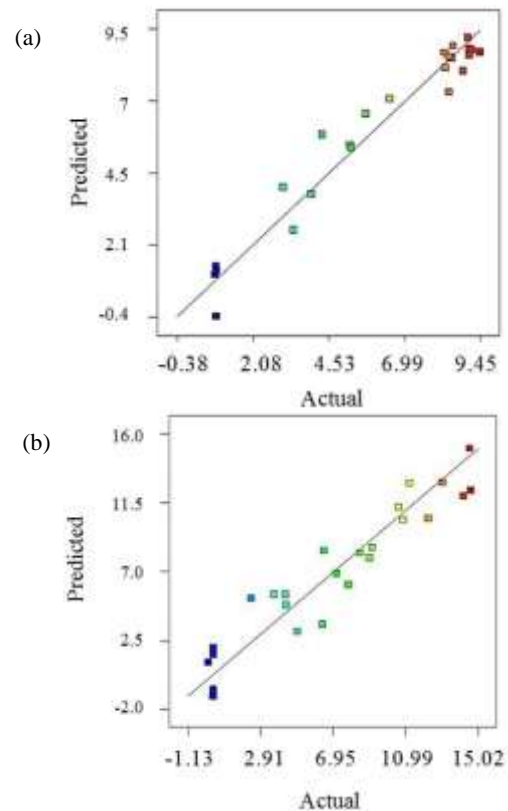


Figure 4. The predicted values of the regression model based on the actual values for; a) the filling percentage of the die, and b) the thinning percentage of the tube

3. 2. Mutual effect of parameters Fig. 5 shows the mutual effect of PX and $P\dot{P}$ on the die filling and tube thinning. Figure 5a indicates the effect of axial feeding on the die filling percentage is enhanced by increasing the pressure. The reason is that the probability of

wrinkling due to increasing the axial feeding is reduced by increasing the pressure. The response surface is dome-shaped shown in Figure 5b, which means that the highest tube thinning is obtained at the center of the surface. Increasing the internal pressure increases the tube thinning, while increasing the axial feeding decreases the tube thinning [10]. Figures 5c and 5d indicate that at low pressure, increasing the pressure rate has no significant effect on the die filling, while it increases the tube thinning sharply. However, at high pressure, increasing the pressure rate decreases both the die filling and tube thinning. It can be due to increasing the probability of bursting at the initial of the deformation.

3. 3. Optimization Optimization was performed to obtain the maximum die filling and the minimum tube

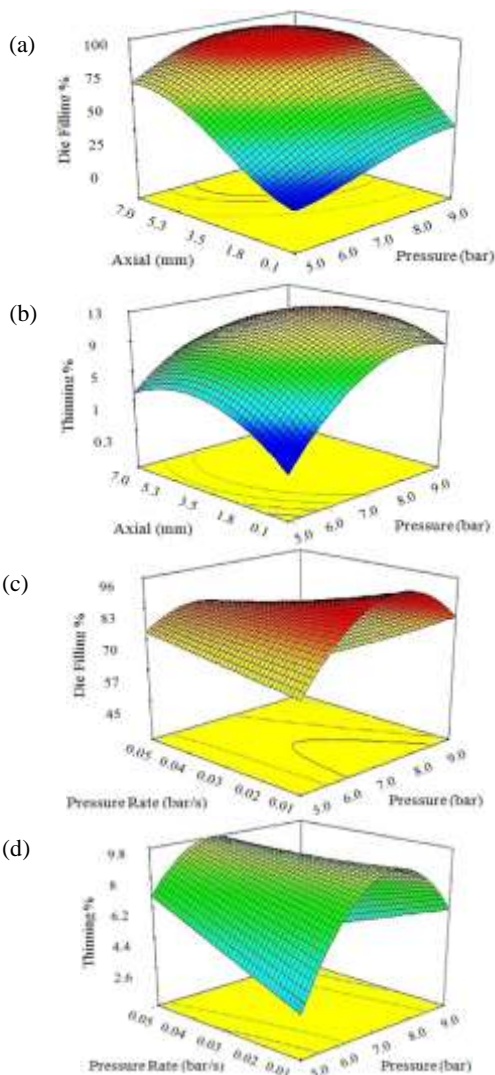


Figure 5. Response surfaces of die filling and tube thinning in terms of input parameters

thinning percentages. The result showed that the optimal loading path was obtained at pressure of 7 bars, pressure rate of 0.01 bar/s, axial feeding of about 7 mm on each side, and a punch speed of 0.02 mm/s. At this condition, the amounts of die filling and tube thinning of 95% and 9.5% were achieved, respectively. Figure 6 shows the loading path obtained from the optimization. It can be seen that the axial feeding reached its maximum value after 350 s and then remained constant by increasing the pressure for 700 s.

Figure 7 shows a cylindrical stepped tube, which formed experimentally using the optimal loading path. The deformation behavior of the tube at different times in the optimal loading path condition is shown in Figure 8. As can be seen, up to 350 s wrinkles were created in the tube due to high axial feeding and low internal pressure, which resulted in a significant amount of the material flowing from the tube edges to the die cavity. Then, by increasing the internal pressure for duration of 700 s, the wrinkles were gradually eliminated, and the die cavity was filled. The internal pressure and axial feeding for different t/d and D/d ratios in the thin-walled tubes range were changed using simulations based on the optimal loading path. Figure 9 shows the perfect specimens, which obtained from experiments for tubes with different t/d and D/d ratios according to the simulations.

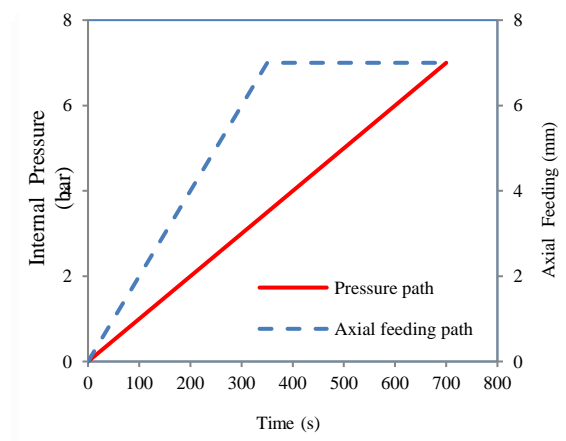


Figure 6. The loading path obtained from the optimization

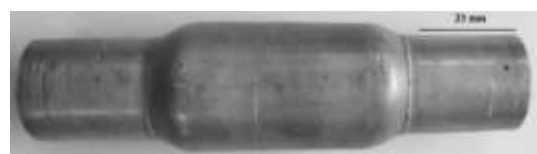


Figure 7. A stepped tube formed with the optimal loading path

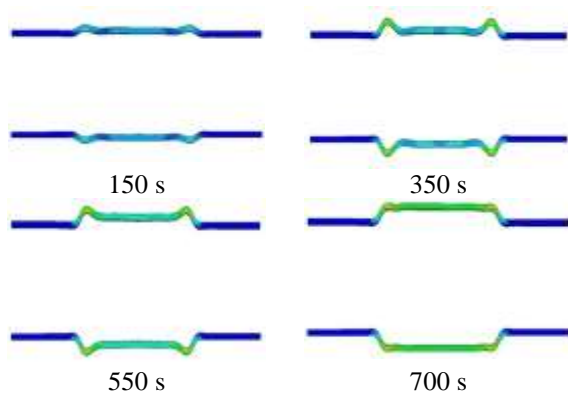


Figure 8. The deformation behavior in the optimal loading path condition

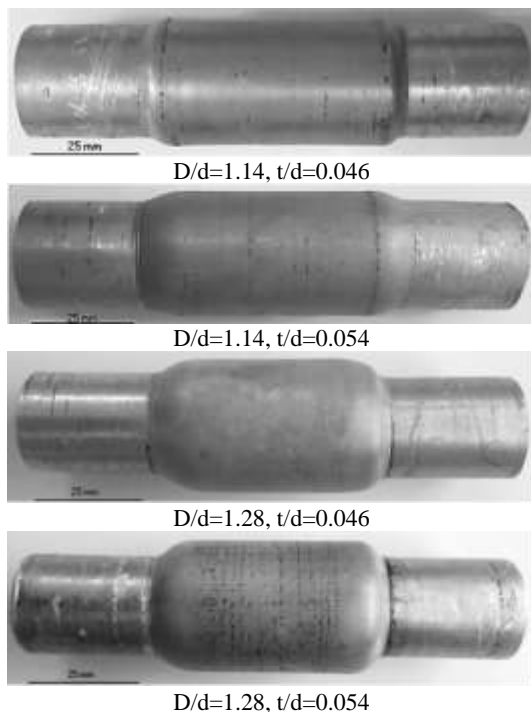


Figure 9. Stepped tubes formed at various D/d and t/d ratios

4. CONCLUSION

A combination of the response surface method and finite element method were used to optimize the loading path of the HMGF process for producing a cylindrical stepped tube from AA6063 alloy at 550 °C. The process variables, including pressure, pressure rate, axial feeding, and punch speed, were investigated to obtain the maximum die filling and minimum tube thinning. The ANOVA results showed that the axial feeding, internal pressure, and their interaction had the most significant effect on the die filling and tube thinning. At low pressure, increasing the pressure rate had no significant effect on the die filling, while it increases the tube thinning sharply. The

optimal parameters were obtained based on the highest die filling rate and the lowest tube thinning at the pressure of 7 bars, pressure rate of 0.01 bar/s, axial feeding of 7 mm from each side, and a punch speed of 0.02 mm/s. At this condition, the amounts of die filling and tube thinning of 95% and 9.5% were achieved, respectively. At optimal loading path, first wrinkles were created in the tube due to high axial feeding and low internal pressure, which resulted in a significant amount of the material flowing from the tube edges to the die cavity. Then, by increasing the internal pressure, the wrinkles were gradually eliminated, and the die cavity was filled.

5. ACKNOWLEDGMENTS

The authors acknowledge Babol Noshirvani University of Technology for the funding and financial support through Grant number BNUT/370203/96.

6. REFERENCES

- Oraon, M., Sharma, V., "Predicting Force in Single Point Incremental Forming by Using Artificial Neural Network", *International Journal of Engineering, Transactions A: Basics*, Vol. 31, No. 1, (2018) 88-95. DOI: 10.5829/ije.2018.31.01a.13
- Tabatabaiea, S. M. R., Alasvand Zarasvand, K., "Investigating the Effects of Cold Bulge Forming Speed on Thickness Variation and Mechanical Properties of Aluminium Alloys: Experimental and Numerical", *International Journal of Engineering, Transactions C: Aspects*, Vol. 31, No. 9, (2018) 1602-1608. DOI: 10.5829/ije.2018.31.09c.17
- Rahmania, F., Seyedkashi, S. M. H., Hashemi, S. J., "Experimental Study on Warm Incremental Tube Forming of AA6063 Aluminum Tubes", *International Journal of Engineering, Transactions C: Aspects*, Vol. 33, No. 9, (2020) 1773-1779. DOI: 10.5829/ije.2020.33.09c.11
- Alijani Renani, H., Haji Aboutalebi, F., "Evaluation of Ductile Damage Criteria in Warm and Hot Forming Processes", *International Journal of Engineering, Transactions A: Basics*, Vol. 29, No. 10, (2016) 1441-1449. DOI: 10.5829/ije.2016.29.10a.15
- Chausov, M., Pylypenko, A., Berezin, V., Volyanska, K., Maruschak, P., Hutsaylyuk, V., Markashova, L., Nedoseka, S., Menou, A., "Influence of dynamic non-equilibrium processes on strength and plasticity of materials of transportation systems", *Transport*, Vol. 33, No.1, (2018) 231-241, DOI: 10.3846/16484142.2017.1301549
- Li, Z., Qu, H., Chen, F., Wang, Y., Tan, Z., Kopec, M., Wang, K., Zheng, K., "Deformation Behavior and Microstructural Evolution during Hot Stamping of TA15 Sheets: Experimentation and Modelling", *Materials* Vol. 12, (2019), 223-236. DOI: 10.3390/ma12020223
- Roohi, A.H., Hashemi, S.J., Allahyari, M., "Hot metal gas forming of closed-cell aluminium foam sandwich panels", *Transactions of the Indian Institute of Metals*, Vol. 73, (2020) 2231-2238. DOI: 10.1007/s12666-020-02027-2
- Paul, A., Werner, M., Tr n, R., Landgrebe, D., "Hot metal gas forming of titanium grade 2 bent tubes", AIP Conference Proceedings, Vol. 1896, (2017), 050009. DOI: 10.1063/1.5008054

9. Mosel, A., Lambarri, J., Degenkol, L., Reuther, F., Hinojo, J., Robiger, L., Eurich, J., Albert, E., Landgrebe, A., Wenzel, D., "Novel process chain for hot metal gas forming of ferritic stainless steel 1.4509", AIP Conference Proceedings, Vol. 1960, (2018), 160019. DOI: 10.1063/1.5035045.
10. Talebi-Anaraki, A., Chougan, M., Loh-Mousavi, M., Maeno, T., "Hot gas forming of aluminium alloy tubes using flame heating", *Journal of Manufacturing and Materials Processing*, Vol. 4, (2020), 56-64. DOI: 10.3390/jmmp4020056
11. Rajaei, M., Hosseini-pour, S.J., Jamshidi Aval, H., "Tearing criterion and process window of hot metal gas forming for AA6063 cylindrical stepped tubes", *International Journal of Advanced Manufacturing Technology*, Vol. 101, (2019), 2609-2620. DOI:10.1007/s00170-018-3052-0
12. Modanloo, V., Alimirzaloo, V., "Minimization of the sheet thinning in hydraulic deep drawing process using response surface methodology and finite element method", *International Journal of Engineering, Transactions B: Applications*, Vol. 29, No. 2, (2016) 264-273. DOI: 10.5829/ije.2016.29.02b.16
13. Mahmood Ali, S., "Optimization of Centrifugal Casting Parameters of AlSi Alloy by using the Response Surface Methodology", *International Journal of Engineering, Transactions B: Applications*, Vol. 32, No. 11, (2019) 1516-1526. DOI: 10.5829/ije.2019.32.11b.02
14. Alaswad, A., Benyounis, K., Olabi, A., "Employment of finite element analysis and Response Surface Methodology to investigate the geometrical factors in T-type bi-layered tube hydroforming. *Advances in Engineering Software*, Vol. 42, (2011), 917-926. DOI: 10.1016/j.advengsoft.2011.07.002
15. Chebbah, M. S., Azaouzi, M., "Geometrical parameters optimization for tube hydroforming using response surface method", AIP Conference Proceedings, Vol. 1618 (2014), 998. DOI: 10.1063/1.4897902.
16. Kadkhodayan, M., Erfani-Moghadam, A., "An investigation of the optimal load paths for the hydroforming of T-shaped tubes", *International Journal of Advanced Manufacturing Technology*, Vol. 61, (2012), 73-85. DOI: 10.1007/s00170-011-3700-0
17. Safari, M., Joudaki, J., Ghadiri, Y., "A Comprehensive Study of the Hydroforming Process of Metallic Bellows: Investigation and Multi-objective Optimization of the Process Parameters", *International Journal of Engineering, Transactions B: Applications*, Vol. 32, (2019), 1681-1688. DOI: 10.5829/IJE.2019.32.11B.19
18. Ahmadi Brooghani, S., Khalili, K., Shahri, S. E., Kang, B., "Loading path optimization of a hydroformed part using multilevel response surface method", *International Journal of Advanced Manufacturing Technology*, Vol. 70, (2014), 1523-1531. DOI: 10.1007/s00170-013-5359-1
19. Huang, T., Song, X., Liu, M., "The multi-objective non-probabilistic interval optimization of the loading paths for T-shape tube hydroforming", *International Journal of Advanced Manufacturing Technology*, Vol. 94, (2018), 677-686. DOI: 10.1007/s00170-017-0927-4
20. Ge, Y., Li, X., Lang, L., Ruan, S., "Optimized design of tube hydroforming loading path using multi-objective differential evolution", *International Journal of Advanced Manufacturing Technology*, Vol. 88, (2017), 837-846. DOI: 10.1007/s00170-016-8790-2
21. Shamsi-Sarband, A., Hosseini-pour, S. J., Bakhshi-Jooybari, M., Shakeri, M., "The effect of geometric parameters of conical cups on the preform shape in two-stage superplastic forming process", *Journal of Materials Engineering and Performance*, Vol. 22, (2013), 3601-3611. DOI: 10.1007/s11665-013-0636-6
22. Hojjati, M., Zoorabadi, M., Hosseini-pour, S. J., "Optimization of superplastic hydroforming process of Aluminium alloy 5083", *Journal of Materials Processing Technology*, Vol. 205, (2008), 482-488. DOI: 10.1016/j.jmatprotec.2007.11.208

Persian Abstract

چکیده

در این مقاله مسیر بارگذاری در فرایند شکل‌دهی فلز داغ با گاز (HMGF) برای ساخت لوله‌های استوانه‌ای پله‌ای از آلایژ آلومینیوم ۶۰۶۳ بهینه‌سازی شد. برای این منظور، از روش‌های سطح پاسخ (RSM) و اجزای محدود (FEM)، به ترتیب به کمک نرم افزارهای دیزاین اسکپرت و آباکوس، استفاده شد. پارامترهای مقدار فشار داخلی، نرخ اعمال فشار، تغذیه محوری و سرعت سنبه بر اساس طراحی آزمایش ترکیبی-مرکزی در سه سطح مورد بررسی قرار گرفت. حداکثر پرشدگی قالب و حداقل درصد نازک شدگی لوله به عنوان توابع هدف انتخاب شدند. تجزیه و تحلیل واریانس نشان داد که تغذیه محوری، فشار داخلی و برهم کنش آنها مهمترین پارامترهای تاثیرگذار در پرشدگی قالب و نازک شدگی لوله می‌باشند. مسیر بارگذاری مطلوب در دمای ۵۵۰ درجه سانتیگراد تحت فشار حدود ۷ بار، نرخ اعمال فشار ۰.۰۱ بار در ثانیه، تغذیه محوری ۷ میلی متر از هر طرف و سرعت سنبه ۰/۰۲۲ میلی متر بر ثانیه بدست آمد. آزمون‌های تجربی آزمایشی برای پارامترهای مشخص شده انجام شد که نتایج بهینه‌سازی را تأیید می‌کند.
